

1
2
3
4
5
6
7
8
9
10
11
12
13
14
15
16
17
18
19

Influence of montmorillonite tactoid size on Na-Ca cation exchange reactions.

Christophe Tournassat^{*}, Mohamed Bizzi, Gilles Braibant and Catherine Crouzet

BRGM, French Geological Survey, Orléans, France

^{*}Corresponding author and mailing address:

Christophe Tournassat

BRGM

Environment and Process Division (EPI/MIS)

3 Avenue Claude Guillemin

45060 Orléans Cedex 2, France

E-mail: c.tournassat@brgm.fr

Tel: +33 (0)2 38 64 47 44

Fax: +33 (0)2 38 64 30 62

1
2
3
4
5
6
7
8
9
10
11
12
13
14
15
16

Abstract

The spatial organisation of swelling clay platelets in a suspension depends on the chemical composition of the equilibration solution. Individual clay platelets can be well dispersed, with surfaces entirely in contact with the external solution, or be stacked in tactoids, where part of the surfaces forms parallel alignments embedding interlayer water and cations. External and interlayer surfaces do not exhibit similar affinities for cations having different hydration and charge properties and the clay platelet stacking arrangement influences the clay affinity for these cations. This paper aims to establish the link between exchange properties and clay tactoid size and organisation for Na-Ca exchange on montmorillonite. Different montmorillonite samples behave differently with regards to Na-Ca exchange, from ideal to non-ideal exchange behaviour. A simple model coupling the tactoid stacking size to different Na/Ca relative affinities of the external and interlayer clay surfaces enables these differences to be reproduced.

KEYWORDS: Cation exchange, montmorillonite, tactoid, stacking, compaction, model

1
2
3
4
5
6
7
8
9
10
11
12
13
14
15
16
17
18
19
20
21
22
23
24
25

1- Introduction

Ion exchange reactions describe the distribution of ions between adsorbed and solution phases. Such reactions have been extensively studied on clay mineral surfaces, where cations counterbalance the intrinsic negative surface charge of these materials. Cation exchange reactions involve major cations from the electrolyte background as well as trace elements in solution. Consequently, cation exchange reactions have for a long time been recognized as of great interest in many fields of investigation. Cation exchange is one of the main factors governing plant nutrient availability, such as potassium in agricultural soils [1-4]. Cation exchange reactions also explain part of the retention properties of clay minerals towards inorganic or organic compounds: heavy metals [5], radionuclides (for instance caesium, [6, 7]), antibiotics in agricultural soils [8, 9], dyes in industrial waste water [10] and other compounds. While clay mineral surfaces have a strong impact on the chemical behaviour of adjacent solutions, solution chemical composition exerts, in turn, a great influence on the physical properties of clay rocks, sediments and soils [11]. For instance, the accumulation of sodium cations in agricultural soils due to poor quality irrigation water is known to be responsible for the destructuration of these soils, reducing their permeability and their mechanical stability [12, 13]. On the other hand, the properties of clay liners used for waste confinement rely heavily on the preservation of their sodic nature, responsible for their low permeability and their semi-permeable membrane behavior [14-16]. These changes in physical properties are linked to the rearrangement of the spatial organisation of swelling clay platelets as a function of chemical conditions from well dispersed clay platelets, whose surfaces are entirely in contact with the external solution, to stacked platelets, where part of the surfaces forms parallel alignments embedding interlayer water and cations. Because external and interlayer surfaces do not *a priori* exhibit similar affinities for cations having

1 different hydration and charge properties, the clay platelet stacking arrangement is expected
2 also to have an influence on the clay affinity for these cations [13, 17]. Given the considerable
3 uncertainty that exists at present regarding the relevance of sorption models calibrated on
4 suspension experiments for further applications in compact clay systems [18-20], it is
5 important to elucidate the link between exchange properties and clay tactoid size and
6 organisation. In this paper, Na-Ca exchange on montmorillonite is investigated as a case
7 study. A reasonable model is constructed that treats adsorption on interlayer and external
8 surfaces as distinct phenomena and satisfactorily describes available ion exchange data.

9

10 **2- Experimental and theoretical background**

11 *2.1- Montmorillonite structure and surface charge*

12 Montmorillonite is built from layers of oxygen atoms and cations (mainly Si^{4+} , Al^{3+} , Mg^{2+} ,
13 Fe^{2+} or $^{3+}$ and H^+) in tetrahedral-octahedral-tetrahedral (TOT) coordination. The TOT layer
14 structure has an excess of negative charge, due to Al for Si substitutions in tetrahedral layers
15 and (Mg , Fe^{2+}) for (Al , Fe^{3+}) substitutions in octahedral layers. The chemical formula of a
16 montmorillonite with both tetrahedral and octahedral substitution is (approximately)
17 $\text{Na}_{0.6}[\text{Si}_{7.8}\text{Al}_{0.2}]^{\text{IV}}[\text{Al}_{3.6}\text{Mg}_{0.4}]^{\text{VI}}\text{O}_{20}(\text{OH})_4$ (omitting water), with molecular weight $MW = 733$
18 g/mol. For a Wyoming MX80 montmorillonite fraction, Madsen [21] reported a MW of 745
19 g/mol. TOT layer negative charge is compensated by hydrated cations (*e.g.* Na^+ , Ca^{2+} , Mg^{2+} ,
20 K^+) in the vicinity of the charged surface (exchanged cations). TOT layers interact to form
21 stacks of layers, hereafter named tactoids. Charge compensating cations can be located in
22 interlayer space, sandwiched between two TOT layers, or on outer surfaces (Figure 1).
23 Typical unit layer charges range from 0.5 to 0.9 per montmorillonite unit cell, equivalent to
24 0.8 to $1.2 \text{ mol}_c \text{ kg}^{-1}$. Outer (A_{ext}) and interlayer (A_{int}) surface area depends on the mean number
25 of stacked TOT layers in tactoids (n_c) according to:

1

$$A_{ext} = \frac{A_{tot}}{n_c}$$

Equation 1

2 and

$$A_{int} = A_{tot} \left(1 - \frac{1}{n_c} \right)$$

Equation 2

3

4 where A_{tot} is the total surface area ($\sim 750 \text{ m}^2 \text{ g}^{-1}$, [21]), neglecting the contribution of

5 terminating edge surface area ($5\text{-}25 \text{ m}^2 \text{ g}^{-1}$, [22-25]). The resulting net structural surface

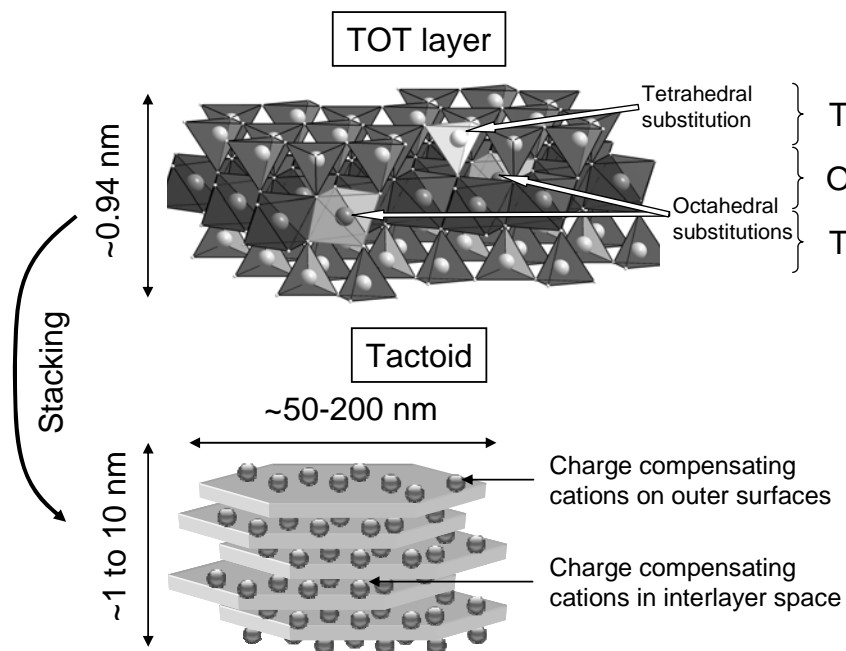
6 charge is $\sigma_0 = -0.1$ to -0.15 C m^{-2} for both types of surface, corresponding to charges typically

7 separated by 10 to 13 Å at the surface. For montmorillonite, the structural charge represents

8 the essential part of the cation exchange capacity (CEC), the variable charge at the broken

9 TOT layer edges accounting for 10% of the total negative surface charge at most [26, 27].

10



11

12

13

Figure 1. Montmorillonite TOT layer and tactoid structures.

1

2 2.2- Na-Ca exchange reaction

3 The exchange process is usually written in the formalism of a chemical reaction [13]. For Na-
4 Ca exchange:



5

6 where X denotes the negatively charged exchange sites that are fully compensated (no free
7 charge) by the exchanged cations. The Na-Ca exchange equilibrium can be expressed as:

$$K_{eq}^{Na \rightarrow Ca} = \frac{(\text{CaX}_2) (\text{Na}^+)^2}{(\text{NaX})^2 (\text{Ca}^{2+})} \quad \text{Equation 3}$$

8 where values in round brackets denote chemical activities. While activity terms for the solute
9 part of the equation are easily obtained through the use of conventional solute activity
10 coefficient computing methods (*e.g.* Davies, Debye-Hückel, Pitzer), the way to describe the
11 activity of exchanged species is more problematic and there is no unifying theory to calculate
12 exchanged species activity coefficients. The exchanger phase is frequently considered as
13 analogous to a solid solution of two (or more) components [13, 28, 29]. In that case, activities
14 of exchanged Na and Ca are expressed as:

$$(\text{CaX}_2) = f_{Ca} N_{Ca} = \frac{[\text{CaX}_2]}{[\text{CaX}_2] + [\text{NaX}]} \quad \text{Equation 4}$$

$$(\text{NaX}) = f_{Na} N_{Na} = \frac{[\text{NaX}]}{[\text{CaX}_2] + [\text{NaX}]} \quad \text{Equation 5}$$

15 where values in square brackets denote concentrations in mol/kg_{clay}, N_i and f_i are respectively
16 mole fractions and rational activity coefficients of the exchanged species i . Introducing
17 Equation 4 and Equation 5 into Equation 3, one obtains:

18

$$K_{eq}^{Na \rightarrow Ca} = \frac{f_{Ca}}{f_{Na}^2} \frac{N_{Ca} (Na^+)^2}{N_{Na}^2 (Ca^{2+})} = \frac{f_{Ca}}{f_{Na}^2} K_v^{Na \rightarrow Ca} \quad \text{Equation 6}$$

1 where K_v is the Vanselow exchange selectivity coefficient [30] that describes an ideal
 2 exchange ($f_i = 1$). The selectivity coefficient can be measured with dedicated batch
 3 equilibration experiments between solution and exchanger (exchange isotherms), but the
 4 rational activity coefficients f_i cannot be directly measured. They can be calculated, together
 5 with the equilibrium constant, as a function of exchanger occupancy based on the exchange
 6 isotherms, but these coefficients, theoretically, cannot be further used for ternary or more
 7 complex exchange systems [28, 31].

8 In practice, cation exchange reactions are evaluated through the calculation of selectivity
 9 coefficients or exchange conditional constants whose definition varies as a function of
 10 empirical conventions. We introduce here, in addition to the Vanselow selectivity coefficient,
 11 the Gaines and Thomas coefficient K_{GT} [32]:

$$K_{GT}^{Na \rightarrow Ca} = \frac{E_{Ca} (Na^+)^2}{E_{Na}^2 (Ca^{2+})} \quad \text{Equation 7}$$

12 where E_i denotes equivalent fraction of species i :

$$E_{Na} = \frac{[NaX]}{2[CaX_2] + [NaX]} \quad \text{and} \quad E_{Ca} = \frac{2[CaX]}{2[CaX_2] + [NaX]} \quad \text{Equation 8}$$

13 The GT coefficient is widely used in the literature for describing exchange reactions on
 14 montmorillonite surfaces. For homovalent exchange (Ca-Mg or Na-K), the GT coefficient is
 15 identical to the Vanselow coefficient but for heterovalent exchange such as Na-Ca exchange,
 16 K_{GT} and K_v are related through:

$$K_{GT}^{Na \rightarrow Ca} = K_v^{Na \rightarrow Ca} \frac{N_{Na}^2}{E_{Na}^2} \times \frac{E_{Ca}}{N_{Ca}} = \frac{4K_v^{Na \rightarrow Ca}}{1 + E_{Na}} \quad \text{Equation 9}$$

17

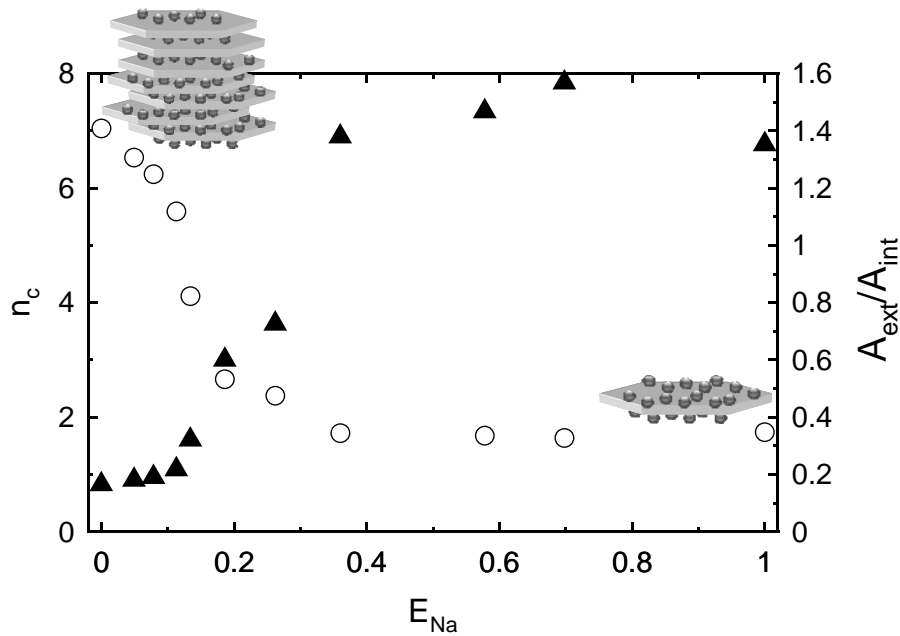
1 Equation 9 shows that if a 1:2 heterovalent exchange reaction (Na-Ca but also Na-Mg, Na-Cu,
2 etc.) behaves like an ideal exchange reaction (constant K_v), then the K_{GT} value decreases from
3 $E_{Na} = 0$ to $E_{Na} = 1$ by a factor of two. For instance, Sposito *et al.* [33] have demonstrated that
4 Na-Cu exchange on Wyoming montmorillonite in perchlorate anionic background is well
5 characterized by a constant Vanselow selectivity coefficient. Sposito and Mattigod [34] have
6 also demonstrated that the apparent changes in K_{GT} for Na – Cu exchange on montmorillonite
7 observed by Maes *et al.* [35] were in fact consistent with a constant Vanselow selectivity
8 coefficient. This statement is also true for Na-Ni and Na-Cd exchange experiments performed
9 by the same authors. However, this is not true for Na-Co and Na-Zn exchange with K_{GT}
10 values varying by a factor of ten from $E_{Na} = 0$ to $E_{Na} = 1$ [35]. Previous studies showed that
11 this variation could be due to the strong pH-dependant adsorption of transition metals on
12 montmorillonite edge surface sites [36]: in that case, this variation should also be observed for
13 Ni, Cu and Cd given the similar affinity of these transition metals for clay edge surfaces [37,
14 38]. Indeed, it has been frequently observed that, independently of the cation exchange
15 scaling convention, the selectivity for divalent cations relative to Na increases with increasing
16 occupancy of the exchanger by the divalent cations [13, 39, 40]. This behaviour has been
17 attributed to contrasted behaviour of interlayer and external surfaces towards cation exchange
18 [41-45] and thus to the formation and destruction of tactoids as a function of experimental
19 conditions.

20

21 *2.3- Influence of exchanged cations on tactoid formation*

22 The mean number of sanded TOT layers in one tactoid depends on the exchanged cations. In a
23 “zero” ionic strength solution, homoionic montmorillonite exchanged with divalent cations
24 (Ca, Mg) tends to form tactoids with n_c values ranging from 4 to 7, while montmorillonite
25 exchanged with monovalent cations (Li, Na, K) exhibits n_c values from 1 to 3 [46-48]. The

1 corresponding ratio of outer to interlayer surfaces (A_{ext}/A_{int}) varies accordingly (Figure 2).
 2 Similar observations were made on Na-Ca clay suspensions in 0.2 mmol/L chloride
 3 electrolyte background [49], but n_c increase started at higher E_{Na} than in the “zero” ionic
 4 strength experiment. Stacking arrangement is thus not only dependent on the exchanged
 5 cations population but also on the ionic strength.

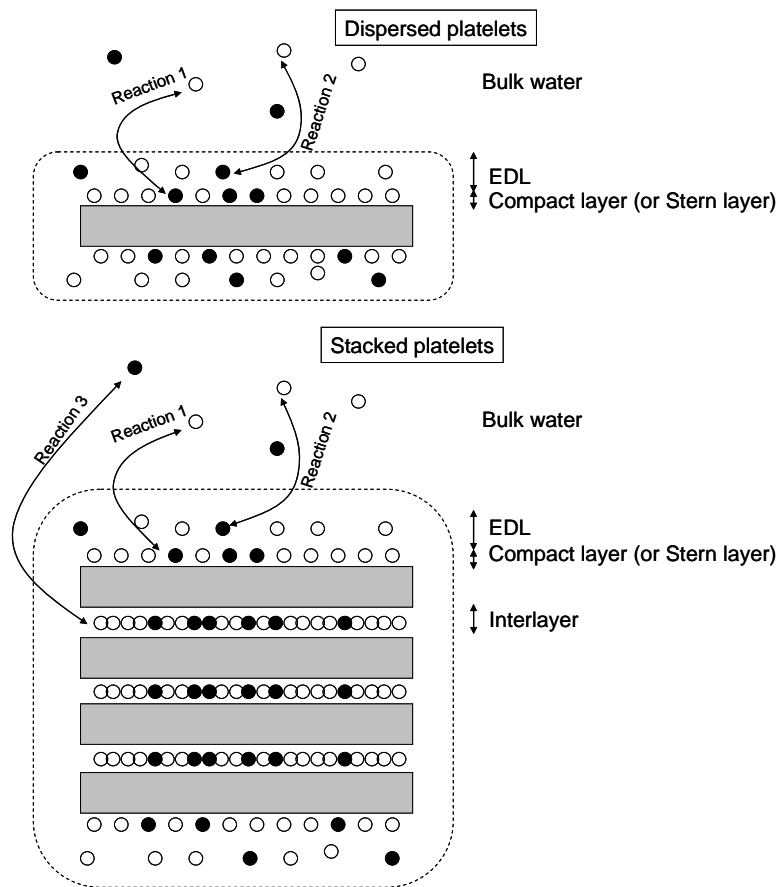


6
 7 Figure 2. Effect of exchanged cations on tactoid formation in a Na/Ca montmorillonite system
 8 at “zero” ionic strength (data from [46]). Circles: change in the number of stacked TOT layers
 9 (n_c) as a function of the relative surface coverage by Na (E_{Na}). Triangles: corresponding ratio
 10 of outer to interlayer surfaces (A_{ext}/A_{int}).

11
 12 *2.4- Distribution of cations on montmorillonite surfaces*

13 The organisation of the solid-solution interface is different at external and interlayer surfaces.
 14 In the interlayer volume, clay structural negative charge is believed to be completely
 15 counterbalanced by exchanged cations. The confined space delimited by the clay surfaces
 16 (typically 6-10 Å, [50, 51]) does not enable the presence of a diffuse layer. On the other hand,
 17 structural negative charge at the external surface is not entirely counterbalanced by cation

1 sorption at the surface and part of the negative charge is screened in the diffuse layer. This
 2 partial compensation of charge can be probed by zeta potential measurements (e.g. [52, 53]).
 3 The distribution of cations on montmorillonite external surfaces cannot be probed directly by
 4 spectrometric methods but molecular dynamic computational methods have made it possible
 5 to show that Na^+ and Ca^{+2} cations are distributed over a compact (or Stern) layer, with outer-
 6 sphere complexes, and the diffuse layer [54, 55]. Only a minor proportion of surface Na^+
 7 cations are engaged in inner-sphere complexes, where Na^+ loses up to three of its hydration
 8 water molecules. This distribution is further assessed qualitatively by analogy with X-ray
 9 reflectivity results on K^+ sorption on muscovite surfaces [56].



10
11

12 Figure 3. Schematic summary of the processes involved in aqueous clay-electrolyte
 13 interactions (modified after [42]). Reaction 1 is an exchange between cations in solution and
 14 cations in the compact (Stern) layer. Reaction 2 is an exchange between cations in solution

1 and cations in the electrostatic diffuse layer (EDL). Reaction 3 is an exchange between
 2 cations in solution and cations in interlayer position.

3
 4 According to the described scheme for cation sorption at montmorillonite interlayer and
 5 external surfaces, at least three types of adsorbed species can be predicted (Figure 3): (i)
 6 diffuse layer cations, (ii) Stern layer cations and (iii) interlayer cations.. The quantitative
 7 importance of these three adsorbed species in the overall measured exchanged selectivity are
 8 expected to vary as a function of the stacking according to the relative external to interlayer
 9 surface area (Equation 1 and Equation 2). Na and Ca sorption can be attributed to the three
 10 adsorbed species according to:

$$q_{Ca} = {}^{int}q_{Ca} + {}^{Stern}q_{Ca} + {}^{DL}q_{Ca} \text{ and } q_{Na} = {}^{int}q_{Na} + {}^{Stern}q_{Na} + {}^{DL}q_{Na} \quad \text{Equation 10}$$

11 where q denotes an equivalent charge (in mol_c/kg clay) and superscripts *int*, *Stern* and *DL*
 12 refer to interlayer, Stern layer and diffuse layer respectively. An effective Vanselow
 13 selectivity coefficient can be expressed for the diffuse layer as well as for the external surface
 14 (taking into account the diffuse layer and the Stern layer):

$${}^{DL}K_v^{Na \rightarrow Ca} = \frac{{}^{DL}q_{Ca} (0.5 {}^{DL}q_{Ca} + {}^{DL}q_{Na}) (Na^+)^2}{2 \times {}^{DL}q_{Na}^2 (Ca^{2+})} \quad \text{Equation 11}$$

$${}^{External}K_v^{Na \rightarrow Ca} = \frac{({}^{Stern}q_{Ca} + {}^{DL}q_{Ca}) (0.5 {}^{Stern}q_{Ca} + 0.5 {}^{DL}q_{Ca} + {}^{Stern}q_{Na} + {}^{DL}q_{Na}) (Na^+)^2}{2 \times ({}^{Stern}q_{Na} + {}^{DL}q_{Na})^2 (Ca^{2+})} \quad \text{Equation 12}$$

15 Equation 12 corresponds to the selectivity coefficient applying to a clay suspension made of
 16 single platelets ($n_c = 1$ where n_c is the mean number of stacked platelet per tactoid,
 17 dimensionless). While it is not possible to measure the contribution of each sorption species
 18 independently, it is possible to make some *a priori* estimates based on available models. For
 19 external surface, we used a modelling approach derived from the model developed by
 20 Dzombak and Hudson [57]. In the following, we make use of the Donnan model to estimate

1 the terms ${}^{DL}q_{Ca}$ and ${}^{DL}q_{Na}$ as a function of ionic strength and the relative concentrations of
 2 cations in solution. According to this model, the mean concentration of a given cation in the
 3 diffuse layer ($c_{D,i}$ in mol/kg_{H2O}) is related to its concentration in the solution phase ($c_{free,i}$ in
 4 mol/kg_{H2O}), its charge (z_i) and a Donnan potential (ψ_D in V) according to [58]:

$$c_{D,i} = c_{free,i} \exp\left(\frac{-z_i F \psi_D}{RT}\right) \quad \text{Equation 13}$$

5 The ions in the diffuse layer balance the charge from the surface:

$$\sum_i z_i c_{D,i} + Q_D = 0 \quad \text{Equation 14}$$

6 where Q_D is the surface charge compensated by the diffuse layer (mol_c kg_{H2O}⁻¹).

7 Neglecting the contribution of anion exclusion, the contribution of Na and Ca cations in
 8 diffuse layer on cation exchange is given by:

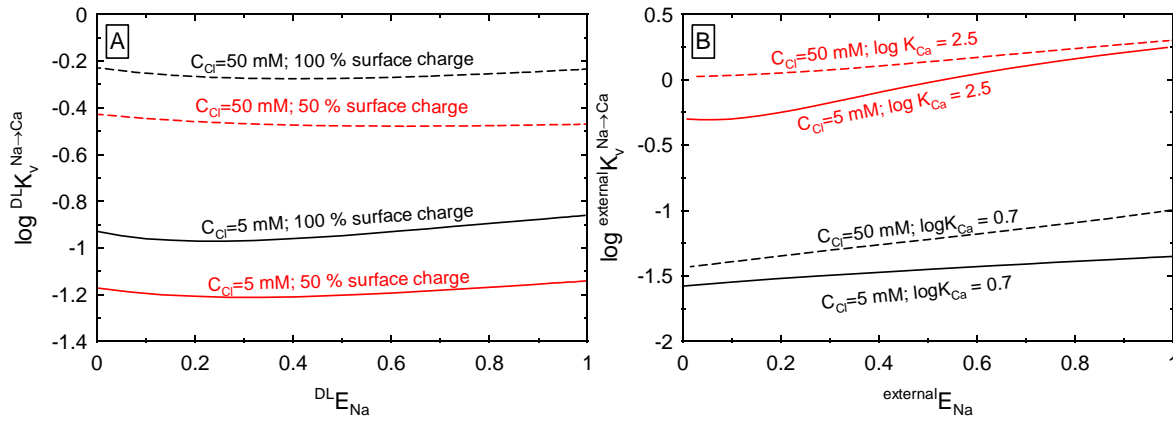
$${}^{DL}q_{Ca} = 2(c_{D,Ca} - c_{Ca}) \times \frac{V_D}{m_{clay}} \quad \text{Equation 15}$$

$${}^{DL}q_{Na} = (c_{D,Na} - c_{Na}) \times \frac{V_D}{m_{clay}} \quad \text{Equation 16}$$

9 where V_D is the considered volume of the diffuse layer (or Donnan volume, in L or kg_{H2O}) and
 10 m_{clay} is the mass of clay (in kg).

11 We considered that the Donnan volume extends up to two Debye lengths from the surface
 12 because, in that case, the calculation of cation excess in the diffuse layer gives nearly identical
 13 results as with the Borkovec and Westall integral method for non-overlapping diffuse layers
 14 [59] but with much better numerical calculation efficiency and speed. We calculated
 15 accordingly the distribution of Ca and Na in the diffuse layer with PHREEQC v2.17,
 16 assuming either (i) a full compensation of the surface charge by the diffuse layer (0.13 C m⁻²)
 17 or (ii) a compensation of only 50% of the surface charge (0.065 C m⁻²). Figure 4 shows that
 18 Na is strongly preferred compared to Ca in the diffuse layer. If the surface charge

1 compensated by the diffuse layer decreases, then the “affinity” for Ca decreases also due to
 2 the increase in surface potential.



3
 4 Figure 4. Na-Ca selectivity coefficient (K_v) at an external montmorillonite surface according
 5 to various hypotheses on ionic strength and Stern and diffuse layer properties. A: effect of the
 6 diffuse layer only (no specific sorption of Na or Ca) on layer selectivity coefficient at two
 7 background chloride concentrations. B: effect of Ca affinity ($\log K_{Ca}$) for the Stern layer on
 8 the external surface selectivity coefficient at two background chloride concentrations (in that
 9 case $\log K_{Na} = 0.8$).

10
 11 The balance of the surface charge over the sites complexed with cations in the Stern layer and
 12 the diffuse layer depends on the affinity of Na for the surface, K_{Na} [60]:

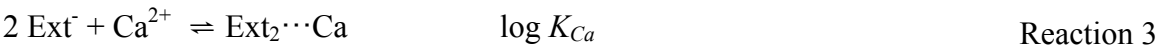


13 where Ext^- denotes a sorption site at the montmorillonite external surface. The value of K_{Na}
 14 cannot be obtained directly from an exchange experiment but can be related to the zeta
 15 potential [61, 62] or calculated theoretically [63]. A large range of K_{Na} values can be found in
 16 the literature depending on the model used (e.g. Basic Stern -BS, Triple Layer Model -TLM,
 17 Double Layer Model -DLM) and the representation of the interface between the clay surface
 18 and the solution [60, 62, 64, 65]. For simplicity reasons, we considered the TLM parameters

1 from [54] (obtained from molecular dynamics calculations combined with zeta potential
2 measurements) and translated them into a single $\log K_{Na}$ DLM parameter ($\log K_{Na} \sim 0.8$).

3 We consider in the following that the sorption of Ca^{2+} on montmorillonite surfaces occurs on
4 the same sorption sites as Na^+ . This representation must be seen as a simplification of the
5 mechanisms, since cations of different nature can (i) be located at different distances from the
6 surface [66] and (ii) have different mobilities and preferential positions with regard to
7 siloxane cavities [67]. For Na-Ca exchange, Bourg and Sposito [55] showed that Na^+ and
8 Ca^{2+} outer-sphere surface complexes are located at essentially identical distances from the
9 smectite surface.

10 We made use of one of the simplest approaches for surface complexation modelling on
11 external surfaces, *i.e.* the electrostatic double layer model as described by Dzombak and
12 Morel [68] and implemented in PHREEQC [69]. In this model, activities of adsorbed species
13 are defined relative to the surface potential of the adsorption plane and surface species
14 occupancy fraction (mole fraction in mol/total moles of sites). This choice aims at having a
15 minimum number of parameters: only the affinity of Ca for the external surface sites, K_{Ca} ,
16 must be fixed:



17 Reaction 3 differs from the reaction described in Dzombak and Hudson [57] where Ca^{2+} was
18 assumed to interact with only a single site ($\text{Ext}^- + \text{Ca}^{2+} \rightleftharpoons \text{Ext} \cdots \text{Ca}^+$) because the mean site
19 spacing in clays (10 to 13 Å, see section 2.1) is much greater than the ionic radius of the Ca^{2+}
20 ion (~ 1 Å). The distribution of charge in clay is however not homogeneous. Charges can also
21 be clustered in some regions of the layer or randomly distributed [70, 71] favouring Ca^{2+}
22 interaction with two charged sites.

1 Of course, the choice of the K_{Ca} value greatly influences the external surface relative affinity
2 for Na and Ca (Figure 4B). If K_{Ca} is sufficiently low ($\log K_{Ca}= 0.7$), the overall affinity of the
3 external surface can be lower than the “affinity” of the diffuse layer for Ca. If K_{Ca} is
4 sufficiently high ($\log K_{Ca}= 2.5$), the diffuse layer has almost no impact on the computed
5 selectivity coefficient. The decrease in ${}^{\text{external}}K_v^{\text{Na}\rightarrow\text{Ca}}$ with increasing Ca population on the
6 exchanger is related to the “mole fraction in mol/total moles of sites” convention used for
7 surface complexation models, which is similar to a Gaines and Thomas scaling convention for
8 cation exchange. Since a Vanselow coefficient is calculated from the results of the
9 complexation model, the constant $\log K_{Na}$ and $\log K_{Ca}$ results in a varying ${}^{\text{external}}K_v^{\text{Na}\rightarrow\text{Ca}}$
10 according to a tendency similar to Equation 9. In both cases (low and high K_{Ca} values), ionic
11 strength has a limited effect on ${}^{\text{external}}K_v^{\text{Na}\rightarrow\text{Ca}}$.

12 According to numerous authors (see discussion in [28]), sites located on interlayer and
13 external surfaces may have unequal cation exchange selectivity, further explaining the
14 existence of exchangeable cations de-mixing, *i.e.* for instance, the preference of Na^+ for
15 external surfaces in a Na-Ca montmorillonite system as probed by electrokinetic
16 measurements [72, 73]. In that case, one expects the selectivity coefficient to vary as a
17 function of E_{Na} because of the accompanying changes in n_c (Figure 2). In the following, we
18 investigate these effects with new measurements in the Na-Ca exchange system and with data
19 available from the literature.

20

21 **3- Material and Methods**

22 *3.1- Solution preparation and concentration measurements*

23 All solutions and suspensions were prepared with Millipore Milli-Q 18 M Ω water. LiCl,
24 NaCl, and CaCl₂ solutions as well as acetic acid/acetate, MES and MOPS buffers were
25 prepared from analytical grade salts. Na, Ca and Cl concentrations were analyzed by liquid

1 ion chromatography (HPLC, Dionex). Na and Ca concentrations were also measured by flame
2 atomic absorption spectrometry (Varian 220FS).

3 3.2- Clay material

4 The fine fraction (<2 µm) of the MX80 natural clay sample material (commercial Wyoming
5 bentonite, reference BF100, CETCO France) was isolated by sedimentation and re-dispersed
6 in NaCl (0.5 mol L⁻¹). It was then successively treated with 0.1 M acetic acid in 0.5 M NaCl
7 (pH ~ 3) to remove carbonate, DCB (dithionite – citrate – bicarbonate) to remove Fe and Mn
8 oxides and finally with 3% H₂O₂, 0.5 M NaCl at 60°C to remove organic matter. Each of the
9 preceding treatments was followed by careful washing with 0.5 M NaCl solution. Finally, the
10 clay was washed three times with NaCl solution (0.05 mol L⁻¹) and stored in the dark at 4°C
11 as a concentrated suspension as recommended by Duc *et al.* [74].

12 3.3- Cation exchange isotherms

13 Na-Ca exchange isotherms were performed at total Cl concentrations ranging from 0.01 to 0.1
14 mol L⁻¹ and solid to liquid ratios from 0.5 to 10 g L⁻¹. The chloride anionic background was
15 preferred to a perchlorate background since it better represents the natural systems studied in
16 our laboratory. The same method as described in Tournassat *et al.* [39] was used to perform
17 exchange isotherms. Equilibration times ranged from 24 to 60 hours, the longer times
18 occurring when the exchange experiments were carried out over a weekend.

19 The amounts of exchanged Na and Ca were calculated with the following formulas:

$$q_{Ca^{2+}} = 2 \times \frac{C_{extr}^{Ca^{2+}} \times (V_{extr} + V_{slurry}) - C_{sol}^{Ca^{2+}} \times (V_{slurry})}{m_{clay}} \quad \text{Equation 17}$$

$$q_{Na^+} = \frac{C_{extr}^{Na^+} \times (V_{extr} + V_{slurry}) - C_{sol}^{Na^+} \times (V_{slurry})}{m_{clay}} \quad \text{Equation 18}$$

1 Where C_{extr}^i is the concentration of cation i measured in the cobalt hexamine extracting
 2 solution (in mol L⁻¹, [75, 76]), C_{sol}^i is the concentration of cation i at equilibrium with the clay
 3 before extraction (in mol L⁻¹), V_{extr} is the volume of extracting solution added to the slurry
 4 after centrifugation (in L), V_{slurry} is the volume of water in the slurry after centrifugation (in
 5 L), and m_{clay} is the mass of clay (in kg).

6 According to the sorption mechanism depicted in Figure 3, part of the water contained in the
 7 clay slurry participates in the hydration of sorbed Na and Ca. As a consequence, we define
 8 adsorption not as a surface excess, but as a kind of partitioning into a distinct "surface water"
 9 phase. The term V_{slurry} should then be corrected from this hydration water contribution. This
 10 correction can be made either by considering that hydration water is mostly interlayer water
 11 or diffuse layer water. We considered that hydration water was mostly diffuse layer water.
 12 Accordingly, we corrected the V_{slurry} term by an amount of water corresponding to a volume
 13 extending up to two Debye lengths from the clay surface (750 m² g⁻¹). In addition to data
 14 obtained for this study, data from [39] were also reprocessed using the same procedure.

15

16 Table 1. Experimental conditions for Na-Ca cation exchange experiments

Series n°	Solid to solution ratio (g/L)	Cl concentration (mol/L)	Final pH range	Conditioning of montmorillonite	Na-
1	0.5	0.01	4.8-5.5	Suspension in NaCl	
2	0.5	0.05	4.7-4.9	Suspension in NaCl	
3	8	0.015	6.9-7.2	Suspension in NaCl	
4	8	0.05	6.7-7.4	Suspension in NaCl	

5	8	0.1	6.7-7	Suspension in NaCl
6*	3	0.005	~5	Dry powder
7*	6	0.005	~5	Dry powder

1 * Experiments from [39]

2

3 3.4- Uncertainties

4 Uncertainties were calculated similarly to Tournassat *et al.* [39] (See electronic annex).

5 3.5- Light transmission measurements

6

7 Light transmission measurements were carried out on suspensions with clay contents ranging
8 from 0.06 to 2 g L⁻¹. Na-conditioned clay was washed twice (3 hours equilibrium and
9 centrifugation) with the solution of interest (LiCl, NaCl, CaCl₂, acetic acid/acetate or MOPS
10 buffer, or a mixture of these solutions at various concentrations). Prior to spectroscopic
11 measurements, the clay suspension was equilibrated 24 hours with the solution of interest,
12 dispersed mechanically and ultrasonicated (3 minutes at 47 kHz). Transmittance data of
13 suspensions were obtained using an Agilent 8453 Spectrophotometer. Measurements were
14 made at the wavelength 650 nm. The absorbance indexes of clay suspensions were measured
15 over the range 200-800 nm. Relative size of tactoids of ionic form *i* and *j* (*N_i* and *N_j*) in
16 suspension were related to their refractive index *K_i* and *K_j* according to [46]:

$$\frac{K_i}{K_j} = \frac{N_i}{N_j} \quad \text{Equation 19}$$

17

18 4- Results

19 4.1- Light transmission measurement results

1 Light transmission measurements enable relative sizes of tactoids in the stacking direction to
 2 be obtained as a function of experimental conditions [46]. The light transmission
 3 measurement results (Table 2) are in close agreement with literature results [46]. Na
 4 montmorillonite suspensions in NaCl 0.01 mol L⁻¹ consist almost of fully dispersed TOT
 5 layers, whereas the presence of Ca in solution promotes the stacking of TOT layers. The
 6 addition of pH buffers (acetic acid/acetate and MOPS) at a concentration of 0.001 mol L⁻¹ had
 7 no marked effect on the stacking of layers.

8
 9

10 Table 2. Tactoid sizes (relative to Li-montmorillonite) inferred from light transmission
 11 measurements in various systems. (AA = acetic acid/acetate buffer).

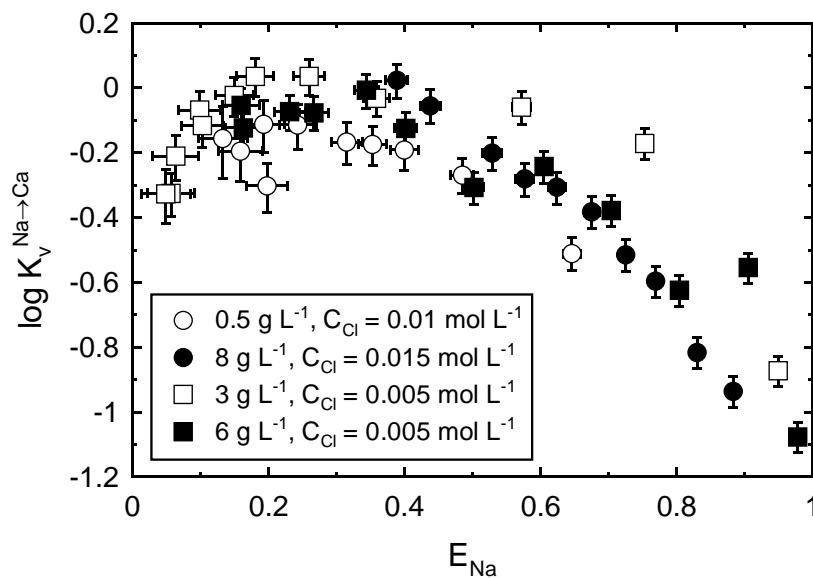
System	Ni/N _{Li}	
	This study	Verburg and Baveye [77]
MX80 + LiCl 0.01M	1	1
MX80 + NaCl 0.01M	1.2-1.3	
Na-MX80 + water (no ionic background)	1.1-1.3	1 -1.7*
MX80 +CaCl ₂ 0.005M	3.1-4.1	2.7->20*
MX80 + NaCl 0.01M + AA 0.001M	1.1-1.9	
MX80 + NaCl 0.01M + MOPS 0.001M	1.4	
MX80 + NaCl 0.01M + CaCl ₂ 0.0001M (E _{Na} ~0.35)	1.5-1.7	
MX80 + NaCl 0.01M + CaCl ₂ 0.0004M (E _{Na} ~0.65)	1.5-2.4	

12 * Most results obtained at “zero” concentration ionic background

13

14 *4.2- Exchange isotherm results*

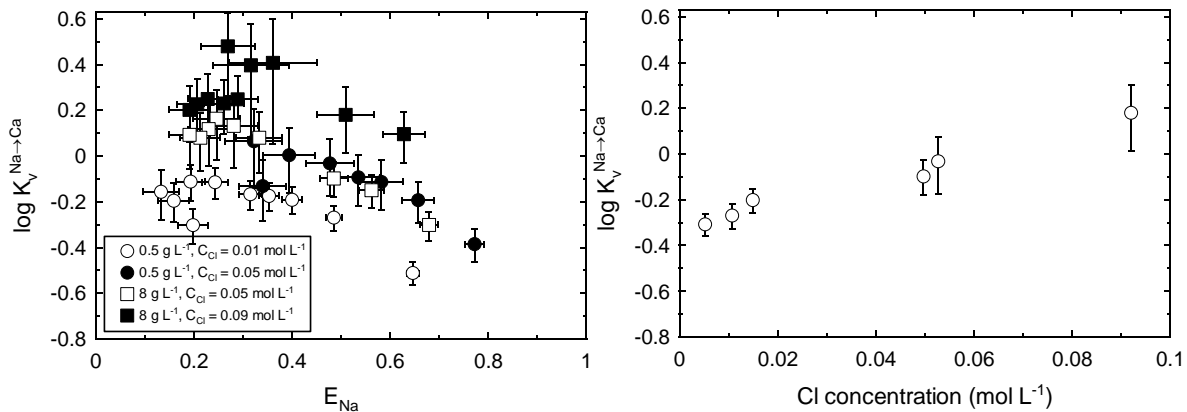
1 Na-Ca cation exchange results for Cl concentration lower than 0.015 mol L^{-1} are shown in
 2 Figure 5, where $\log_{10} K_v^{Na \rightarrow Ca}$ is plotted as E_{Na} . No clear trend in the dependency of the cation
 3 selectivity coefficient as a function of the solid to liquid ratio from 0.5 to 8 g L^{-1} can be
 4 observed while Tertre et al. observed such an effect from 2.5 to 25 g L^{-1} [78]. For all
 5 conditions, the Na-Ca selectivity coefficient is almost constant (in the limit of data
 6 repeatability) from $E_{Na} = 0.2$ to $E_{Na} = 0.4-0.6$ and then decreases continuously up to $E_{Na} = 1$
 7 but experimental results are more scattered for $E_{Na} > 0.6$ than for $E_{Na} < 0.6$. The same trend is
 8 also observed for experiments performed at higher chloride concentration but with selectivity
 9 coefficient values higher than those measured at low Cl concentration (Figure 6). If the GT
 10 selectivity coefficient is considered in place of Vanselow, the same trend is observed (not
 11 shown). We conclude (i) that in our experiments the solid to liquid ratio has almost no
 12 influence on the measured selectivity coefficient, (ii) that the increase in chloride background
 13 concentration causes an increase in the Na-Ca selectivity coefficient and (iii) that the changes
 14 in selectivity coefficient as a function of E_{Na} are not due to the choice of cation exchange
 15 scaling convention in the investigated systems.



16

1 Figure 5. Na-Ca exchange experiment results as a function of solid to liquid ratio for low Cl
2 concentration ($C_{Cl} < 0.015$ mol/L).

3
4
5



6
7 Figure 6. Left: Na-Ca exchange selectivity coefficient as a function of ionic strength and solid
8 to liquid ratio. Right: Na-Ca exchange selectivity coefficient as a function of ionic strength
9 for $E_{Na} \sim 0.5$.

10

11 5- Discussion and modelling

12 5.1 Comparison with literature data

13 Available Na-Ca exchange data from the literature are shown in Figure 7. If possible, K_v
14 values were recalculated from tabulated solution and exchanger composition ([45, 79, 80] and
15 [81], the latter reference giving exchange results in the system Na-Ca/Mg). In some cases,
16 solution and exchanger phase composition were derived from exchange isotherm figures and
17 information on the anionic salt concentration [82]. Otherwise, selectivity coefficient values
18 were directly scanned from reference figures and if needed reprocessed as Vanselow
19 selectivity coefficients instead of GT selectivity coefficients according to Equation 9 [43, 83-

1 85]. Error bands were not calculated due to a lack of available data for most of the
2 experiments

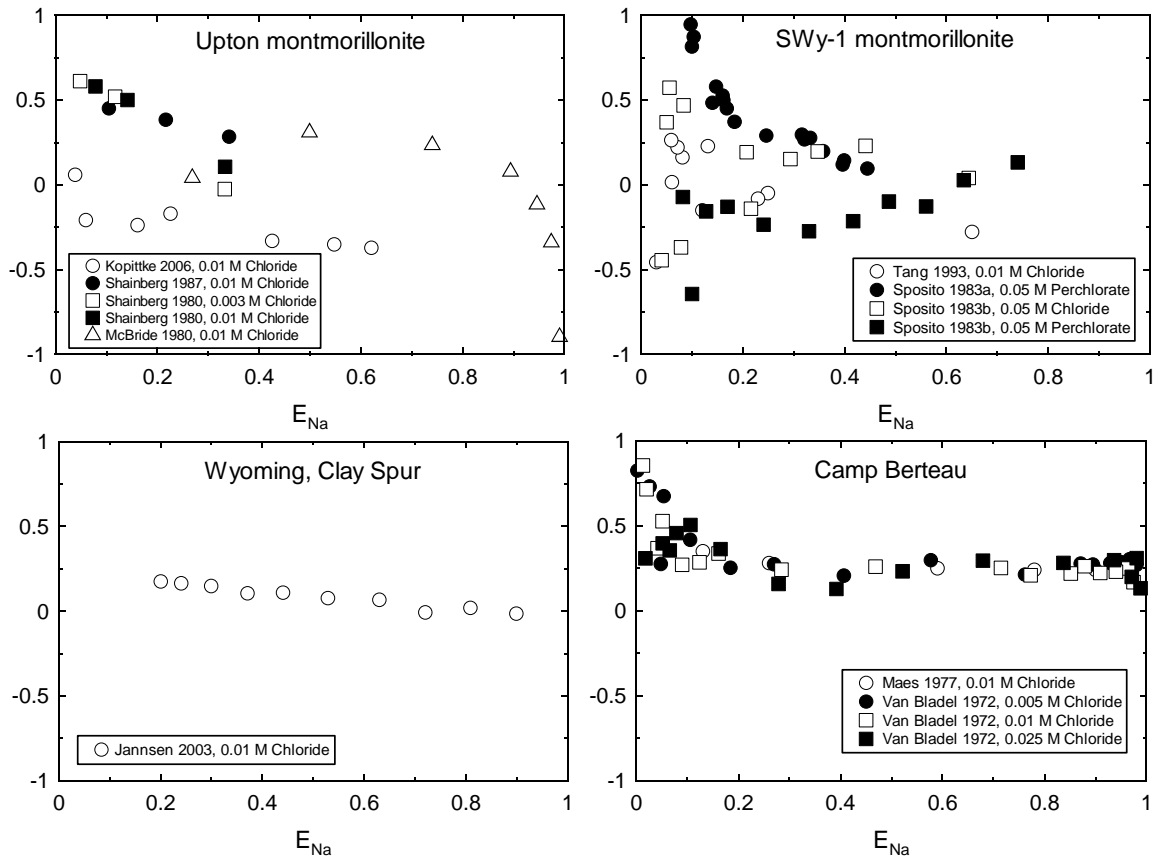
3 Depending on the clay, the measured selectivity coefficients do not cover the same range of
4 values. For a given clay, the measured selectivity coefficients vary by 0.5 log units from one
5 study to the next (*e.g.* Upton montmorillonite). The lack of measurement reproducibility can
6 be due, at least, to (i) different surface properties for measurements on different clays (surface
7 charge, distribution of charges on tetrahedral and octahedral sites for instance, [86]) (ii)
8 differences in measurement methods or natural heterogeneity of the clay samples for clay of
9 the same origin. Despite these limitations, available literature data make it possible to
10 distinguish at least two types of contrasting behaviour.

11 (i) Na-Ca exchange on Camp Berteau montmorillonite is nearly ideal in the E_{Na} range
12 0.1-1. For $E_{Na} < 0.1$, the apparent increase in the selectivity coefficient value is not
13 clear due to dispersion of the data.

14 (ii) Na-Ca exchange on Upton montmorillonite shows a tendency of selectivity
15 coefficient decrease with increasing E_{Na} . This montmorillonite sample is also the
16 only one we found that exhibits very low selectivity coefficient at $E_{Na} \sim 1$, similarly
17 to the MX80 sample we used ($\log K_v^{Na \rightarrow Ca} < -0.8$ at $E_{Na} \sim 1$). The Wyoming Clay
18 Spur sample also shows a tendency of selectivity coefficient decrease with
19 increasing E_{Na} , although the K_v variation is limited to 0.2 log units.

20 For Swy-1 montmorillonite, the dispersion in the results and the lack of data at $E_{Na} > 0.8$ does
21 not make it possible to choose between these two options, ideal exchange vs. decreasing
22 affinity for Ca as a function of Na exchanger occupancy. Baeyens and Bradbury [87]
23 measured the distribution coefficient of Ca on Na-Swy-1 at trace concentration of Ca (*i.e.* E_{Na}
24 = 1) with radiotracer techniques. Their distribution coefficient corresponds to a Vanselow
25 selectivity coefficient of 0.03 ± 0.07 in log scale. This distribution coefficient was measured

1 at pH between 5 and 9 using pH buffers. The possible effect of these buffers on the TOT layer
 2 stacking was evaluated through light transmission measurements (Table 2) and we found no
 3 marked effect of their use. As a result, Na-Ca selectivity coefficient on Swy-1 at high E_{Na}
 4 seems to follow a similar trend as on Camp Berteau montmorillonite, i.e. ideal exchange at
 5 high E_{Na} .



7
 8 Figure 7. Na-Ca exchange selectivity coefficient as a function of sodium exchanger
 9 occupancy for various clays studied in the literature.

10

11 5.2- Possible sources of experimental artefact

12 The very low value of our selectivity coefficients at an E_{Na} value close to 1 and more
 13 generally the low $\log K_v$ values in the whole exchanger composition domain is unusual.
 14 According to Figure 7, such negative values in the montmorillonite Na-Ca system are very
 15 seldom reported (see [43] and, to a lesser extent, [83] for $E_{Na} < 0.6$ with no value available at
 16 higher E_{Na}). This statement casts some doubts on the representativeness of the data obtained

1 in this study, although the repeatability of the results with regard to the results we obtained in
2 2009 [39] is good despite the use of a new MX80 clay stock. Sources of artefacts must then
3 be discussed.

4 Discrepancies in results could result from various causes including experimental measurement
5 artefacts such as incomplete recovery of exchangeable Ca^{2+} upon extraction by cobalt
6 hexamine or insufficient reaction time. The first hypothesis is however not realistic: (i) the
7 ability of the cobalt hexamine method to measure accurately cation exchange composition has
8 been demonstrated repeatedly [75, 76, 88, 89]; and (ii) the amount of exchanged Ca^{2+} with the
9 cobalt hexamine method compares well with the amount of exchanged calcium calculated
10 from initially added and final Ca concentration in the solution (not shown).

11 Insufficient experimental reaction time must also be ruled out. $\text{Na} \rightarrow \text{Ca}$ cation exchange
12 reactions on montmorillonite are fast reactions [82] and our experimental equilibration time
13 lasted at least 24 hours, similar to the Sposito *et al.* study [33]. Tertre *et al.* showed that there
14 was no difference between experiments lasting three days or one week. Baeyens and
15 Bradbury [87] evaluated the distribution coefficient of Ca at trace concentration on Swy-1
16 montmorillonite and could not detect significant changes between one day and three weeks.

17 One other source of error could be linked to the uncertainty of the measurement at high E_{Na} .
18 However, the extent of calculated error bands enables this hypothesis to be discarded. An
19 error of 1 log unit for K_v would correspond to a tenfold error on the Ca concentration or on
20 the amount of exchanged Ca. Both hypotheses are clearly not reasonable. As a consequence,
21 present evaluation of the data shows that the large changes in selectivity coefficient and its
22 very low minimum value are certainly not due to experimental artefacts or measurement
23 uncertainties. The scatter of data in some conditions must consequently be attributed to
24 variability in response of the system. However, discrepancies in the observed trends with
25 other literature data still need to be elucidated.

1
2
3
4
5
6
7
8
9
10
11
12
13
14
15
16
17
18
19
20
21

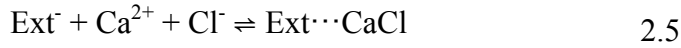
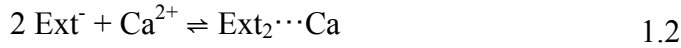
5.3- Coupling tactoid formation to cation exchange mechanism

The experimental data shown in Figure 5 were reproduced using a model combining cation exchange in interlayer and surface complexation at the external surfaces. Fitting model parameters were (i) the affinity of Ca relative to Na for the interlayer ($\log K_v^{int}$ assumed constant), (ii) the affinity of Ca for the external surface ($\log K_{Ca}$) and (iii) the stacking size of tactoids (n_c). The maximum n_c value was fixed at 4.1 according to the results shown in Table 2 for the MX80 + CaCl₂ 0.005 mol L⁻¹ system. The affinity of Ca for the external surfaces ($\log K_{Ca}$) was obtained from experimental points at $E_{Na} \sim 1$ where no or little stacking of clay platelet was awaited ($n_c \sim 1.1-1.2$ see Table 2). Then, the affinity of Ca for internal surfaces was obtained from data at low E_{Na} with $n_c \leq 4.1$. Once these two values were obtained, data were fitted by adjusting n_c for each data point. n_c values at intermediate exchanger composition ($E_{Na} \sim 0.35$ and 0.65) were compared to those obtained from light transmission measurements (Table 2) and the affinities of Ca for internal and external surfaces were repetitively readjusted to better match these intermediate values. Data at higher salt concentration (Figure 6) were then fitted by adding an additional contribution from the sorption of CaCl⁺ ion pairs on the clay external surfaces [39, 78, 90-92]. Model parameters are given in Table 3 and fitted n_c values are plotted in Figure 8 and Figure 9 together with the comparison between measured and calculated selectivity coefficient values.

Table 3. Cation exchange model parameters.

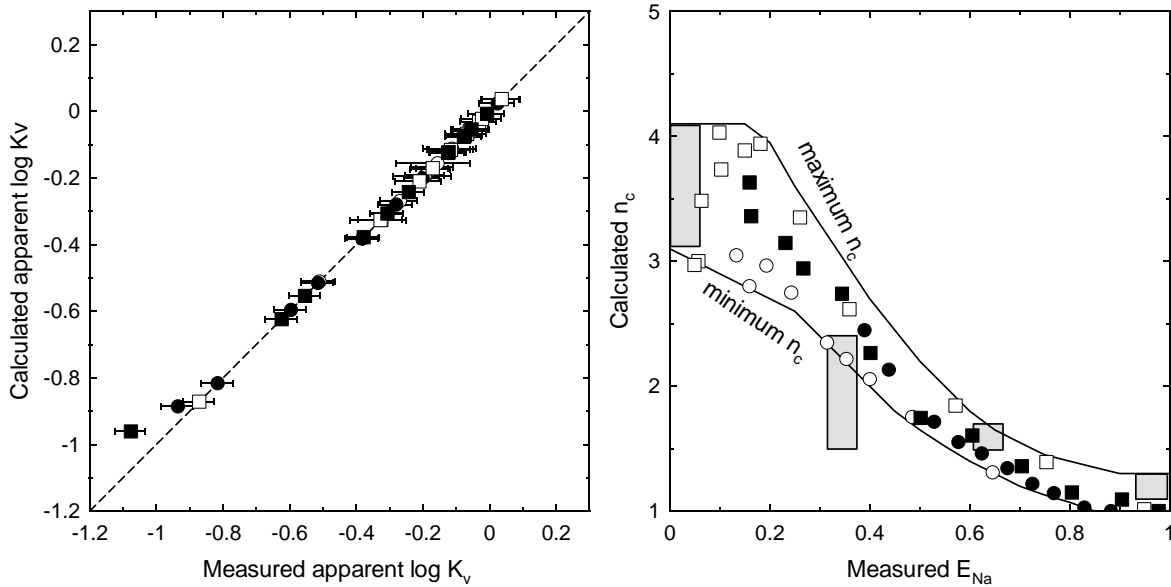
Reaction	log K
<i>Interlayer</i>	
$2 \text{IntNa} + \text{Ca}^{2+} \rightleftharpoons \text{Int}_2\text{Ca} + 2 \text{Na}^+$	1 (Vanselow)

Outer surfaces



1

2



3

4 Figure 8. Left: comparison between experimental and model results for data at low salt

5 concentration (open circles: system 1; closed circles: system 3; open squares: system 6; closed

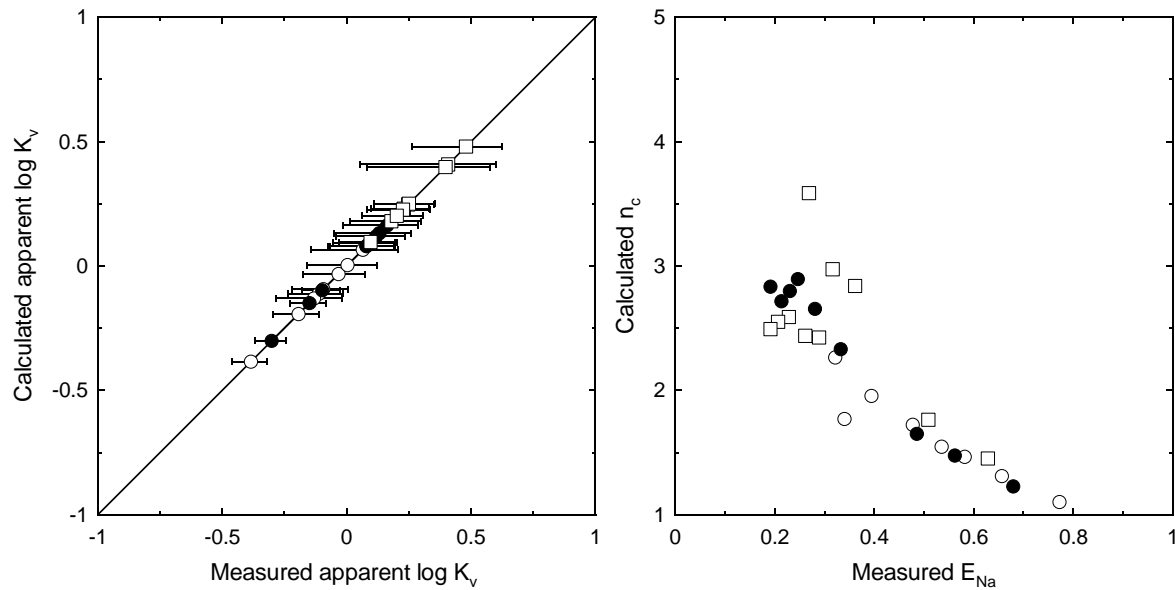
6 squares: system 7; see Table 1 for details; the straight line is the 1:1 relationship). Right:

7 corresponding stacking number n_c as a function of Na occupancy on the exchanger. The plain

8 lines in the right figure denote the envelope of n_c values. The gray areas are representative of

9 n_c value deduced from light transmission measurements (Table 2).

1



2

3 Figure 9. Left: comparison between experimental results and model for data at high salt
4 concentration (open circles: system 2; closed circles: system 4; open squares: system 5; see
5 Table 1 for details; the straight line is the 1:1 relationship). Right: corresponding stacking
6 number n_c as a function of Na occupancy on the exchanger.

7

8 Experimental results (apparent log K_v values) are well reproduced by the model. It can be
9 argued, however, that the model parameter set is certainly not unique. In the proposed model
10 (Table 2), Ca affinity for external surfaces is lower than Na affinity ($\log K_{Ca} - 2 \log K_{Na} = -$
11 0.4). McBride [13] pointed out that montmorillonite charge sites are typically separated by 10
12 to 15 Å, favouring Na^+ as compared to Ca^{2+} for electrostatic bonds at the external surfaces.
13 Differences in structural charge distribution and location in the TOT layer of montmorillonite
14 samples [70, 71], correlated to differences in electrostatic terms and/or configurational
15 entropy changes [13], could be reflected in turn in the K_{Na} and K_{Ca} value of the present
16 model. Ideally, these values should be obtained by measurements independent of cation
17 exchange isotherms on various clay samples exhibiting contrasting Na-Ca exchange

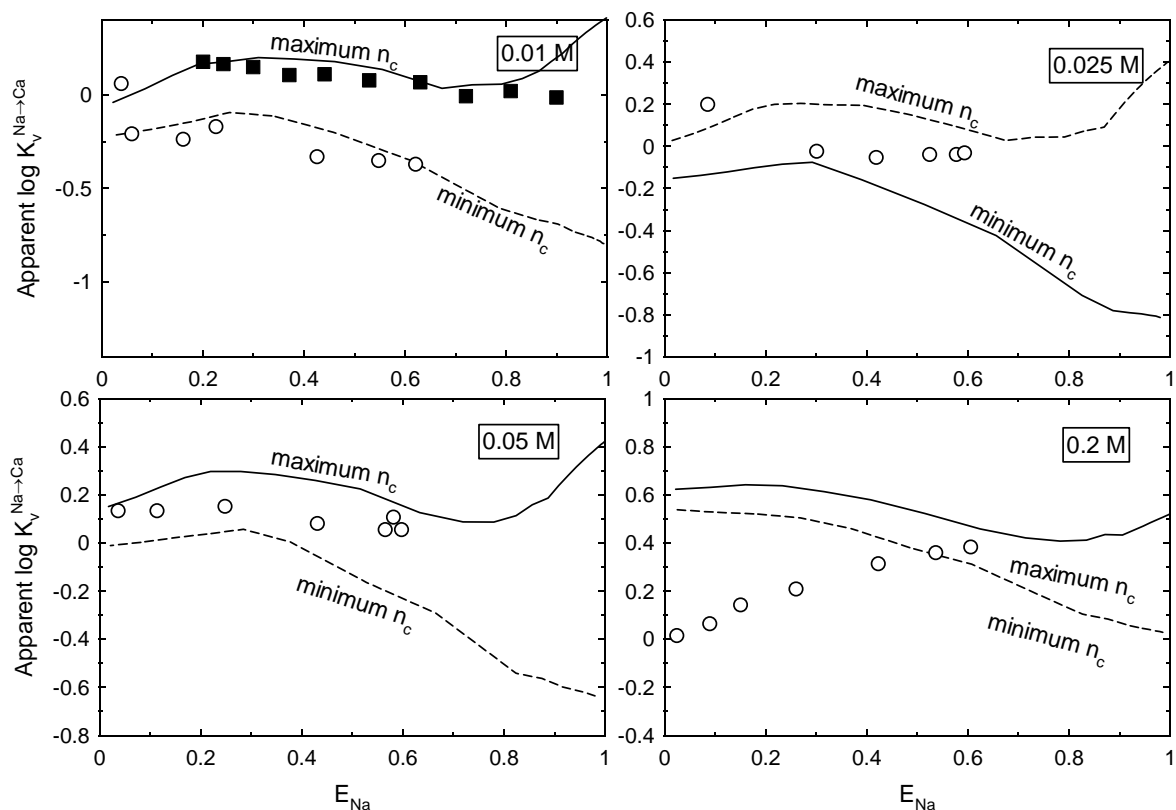
1 behaviour. The evolution of n_c as a function of E_{Na} is not found to be identical to that depicted
2 in Figure 2 but is in relative good agreement with values obtained in the present study at E_{Na}
3 ~ 0.35 and 0.65 . According to Verburg and Baveye [77], n_c values can differ significantly
4 from one experiment to another as a function of the suspension preparation procedure and
5 ionic strength. For instance, Lahav and Bannin [49] showed a gradual increase in the
6 absorbance index ratio from $E_{Na} = 0$ to $E_{Na} = 0.5$ and then a sharp increase in this index ratio
7 from $E_{Na} = 0.5$ to $E_{Na} = 0.15$ in a Na/Ca montmorillonite exchange experiment performed at
8 0.2 mmol/L Cl background electrolyte concentration. The important point, here, is that n_c
9 changes as a function of E_{Na} are consistent with existing data: the minimum value of n_c at E_{Na}
10 ~ 1 is slightly above 1, and the maximum n_c value at $E_{Na} \sim 0$ is about 4, in close agreement
11 with measured values reported (Table 2). Moreover, the increase in n_c is enhanced at an E_{Na}
12 value below 0.4 , also in agreement with literature data [46, 48, 93]. As a consequence, tactoid
13 formation upon sorption of Ca on clay surfaces can account for the observed cation selectivity
14 changes as a function of exchanger composition.

15

16 5.4- Application to literature data

17 The model with parameters given in Table 3 was applied to literature data and with minimum
18 and maximum n_c values given by the envelope of values shown in Figure 8 (“minimum and
19 maximum n_c ”). Data from Kopittke *et al.* [83] are correctly reproduced by the model as a
20 function of ionic strength. At 0.01 mol/L chloride electrolyte background, data are best
21 reproduced using the minimum n_c curve (Figure 8), while at 0.025 and 0.05 M Cl electrolyte
22 background, data are best reproduced with n_c values in-between minimum and maximum n_c
23 curves. At 0.2 M Cl, the model fails to reproduce the measured trend of selectivity coefficient
24 variation. However, in these conditions, one expects large error bands on the experimental
25 data (see Figure 6). The model is also in near agreement with data from Jannsen *et al.* [84] if

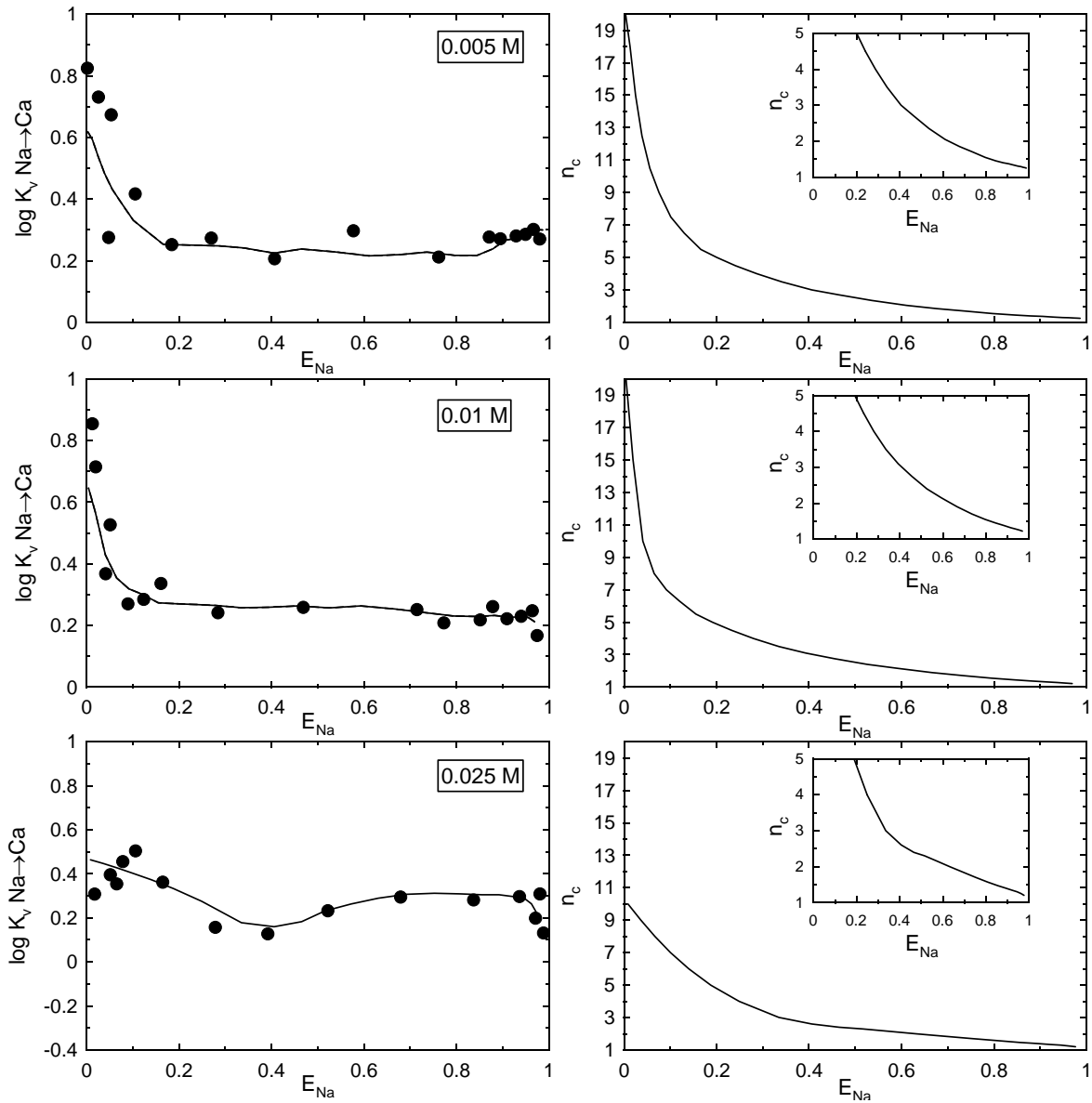
1 the maximum n_c curve is considered. These model predictions can also be used to see how
 2 sensitive the model is to the choice of n_c value: up to one order of magnitude difference is
 3 obtained in apparent $\log K_v^{Na \rightarrow Ca}$ when a n_c value of 1 is chosen in place of a n_c value of 1.3 at
 4 E_{Na} value close to 1. It may also be seen that using the maximum n_c curve as an input
 5 parameter enables $\log K_v^{Na \rightarrow Ca}$ variations accounting for less than 0.3 log units to be obtained.
 6



7
 8 Figure 10. Comparison of model prediction using parameters from Table 3 with data from
 9 Kopitke *et al.* ([83], open circles) and Jannsen *et al.* ([84], black squares). “Maximum” and
 10 “minimum n_c ” refer to the n_c envelope curves shown in Figure 8.

11
 12 Data obtained on Camp Berteau montmorillonite [85, 86] with an almost constant selectivity
 13 coefficient value (~ 0.3) could not be predicted by the model without raising the n_c values
 14 above the maximum values shown on Figure 8. A n_c value of ~ 20 was necessary to reproduce

1 experimental data at low E_{Na} (Figure 11). Although this value is far higher than the value
2 obtained in the present study for MX80 montmorillonite, it is still in agreement with other
3 values reported in the literature (Table 2, [77]). The speed of shaking and the volume of
4 suspension per flask significantly affect the thickness and lateral extent of the quasi-crystal
5 [77, 94]. Impurities such as adsorbed Al^{3+} could also play a role by influencing the stacking
6 arrangements of montmorillonite lamellae [90]. As a consequence, observed differences
7 amongst published cation exchange data could be due to differences in platelet stacking
8 during the experiments. This platelet staking effect has already been proved for the Mg-K
9 exchange reaction on montmorillonite where forward reaction (Mg replaced by K) and
10 backward reaction (K replaced by Mg) did not lead to identical exchange selectivity
11 coefficients [11]. Moreover, the selectivity coefficients evolved slowly with time and this
12 evolution was correlated with a change in tactoid size. The present modelling study shows
13 that this effect may also be true for Na-Ca and other monovalent-divalent exchange reactions.
14 The main difficulty arising from this modelling analysis is the absence of a unique set of
15 parameters reproducing the data for Na-Ca exchange on various montmorillonite samples.



2

3 Figure 11. Comparison of data from Van Bladel *et al.* on Camp Berteau montmorillonite
 4 ([85], circles on left figures) model (plain lines on left figures) using adjustable n_c values (right
 5 figures).

6

7

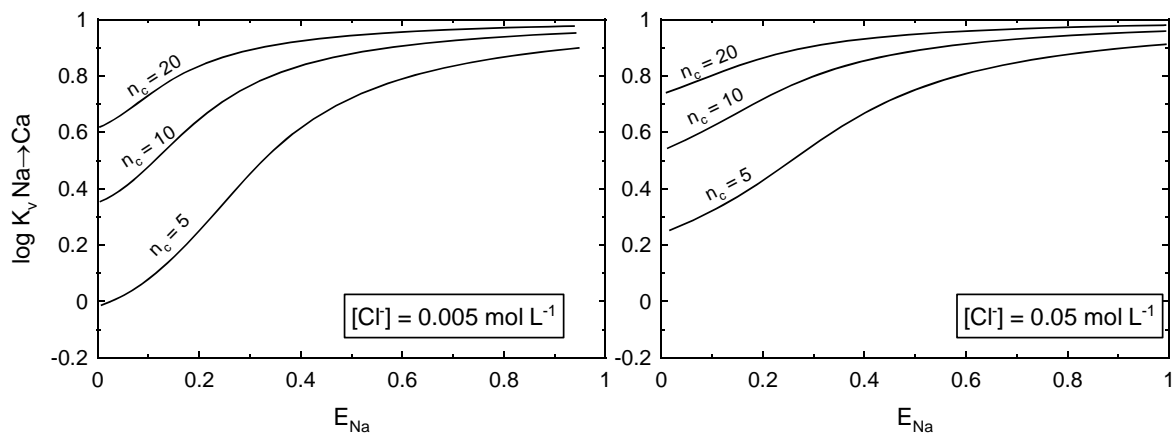
8

9

1 5.5- Implications for cation exchange in compacted systems (clayrocks, sediment, soils)

2 The effect of tactoid size implies that selectivity values obtained for heterovalent cation
3 exchange (Na-Me²⁺, where Me stands for a divalent cation) in laboratory experiments could
4 not be directly transferable to natural systems. Natural clay systems (clayrocks, sediments or
5 soils) exhibit textural properties that can differ from dilute suspensions: in particular, higher
6 n_c values are expected due to compaction of the material [95]. Figure 12 shows the effect of
7 ionic strength and compaction on the apparent Na-Ca selectivity coefficient calculated with
8 the present model ($n_c = 5, 10$ and 20 for illustrative purposes, [11, 96]). If parameters are
9 taken from Table 3, then the apparent selectivity coefficient value varies from 0 to 1 as a
10 function of compaction, ionic strength and exchanger composition.

11



12

13 Figure 12. Effect of stacking due to compaction (n_c) and ionic strength on the apparent Na-Ca
14 selectivity coefficient..

15

16 **Conclusions**

17 We have shown that different montmorillonite samples behave differently with regards to Na-
18 Ca exchange, from ideal to non-ideal exchange behaviour. Exchange data can be reproduced
19 by a model coupling the tactoid stacking size to different Na/Ca relative affinities of the
20 external and interlayer clay surfaces. According to this model, clays would have low affinity

1 for Ca on their external surfaces. This result has implications on the applicability of
2 selectivity coefficients determined from experiments in dispersed suspension for the
3 prediction of compacted clay-rock properties where the effect of platelet stacking should be
4 taken into account.

5

6 **Acknowledgments**

7 The results presented in this article were collected during the GL-Transfert project funded by
8 ANDRA in the framework of the ANDRA/BRGM scientific partnership. Ian Bourg and an
9 anonymous reviewer are gratefully acknowledged for their constructive comments.

2 **References**

- 3 1. S. Feigenbaum; A. Bar-Tal; R. Portnoy; D. L. Sparks, *Soil Sci. Soc. Am. J.* **1991**, 55,
4 49-56.
- 5 2. P. M. Jardine; D. L. Sparks, *Soil Sci. Soc. Am. J.* **1984**, 48, 45-50.
- 6 3. S.-I. Wada; K. Odahara, *Soil Sci. Plant Nutr.* **1993**, 39, (1), 129-138.
- 7 4. J. O. Agbenin; S. Yakubu, *Geoderma* **2006**, 136, (3-4), 542-554.
- 8 5. A. Weiss; G. C. Amstutz, *Miner. Deposita* **1966**, 1, 60-66.
- 9 6. C. Liu; J. M. Zachara; S. C. Smith, *J. Contam. Hydrol.* **2004**, 68, (3-4), 217-238.
- 10 7. M. H. Bradbury; B. Baeyens, *J. Contam. Hydrol.* **2000**, 42, (2-4), 141-163.
- 11 8. M. E. Essington; J. Lee; Y. Seo, *Soil Sci. Soc. Am. J.* **2010**, 74, (5), 1577-1588.
- 12 9. L. A. Pinck, *Clay. Clay. Miner.* **1960**, 9, 520-529.
- 13 10. P. Liu; L. X. Zhang, *Sep. Purif. Technol.* **2007**, 58, (1), 32-39.
- 14 11. K. Verburg; P. Baveye; M. B. McBride, *Soil Sci. Soc. Am. J.* **1995**, 59, (5), 1268-1273.
- 15 12. J. P. Quirk, *Aust J Soil Res* **2001**, 39, (6), 1185-1217.
- 16 13. M. B. McBride, *Environmental Chemistry of Soils*. Oxford University Press: New
17 York Oxford, 1994.
- 18 14. D. Guyonnet; E. Gaucher; H. Gaboriau; C. H. Pons; C. Clinard; V. Norotte; G. Didier,
19 *J. Geotech. Geoenviron.* **2005**, 131, (6), 740-749.
- 20 15. D. Guyonnet; N. Touze-Foltz; V. Norotte; C. Pothier; G. Didier; H. Gailhanou; P.
21 Blanc; F. Warmont, *Geotext. Geomembranes* **2009**, 27, (5), 321-331.
- 22 16. C. D. Shackelford; J. M. Lee, *Clay. Clay. Miner.* **2003**, 51, (2), 186-196.
- 23 17. D. A. Laird; C. Shang, *Clay. Clay. Miner.* **1997**, 45, (5), 681-689.
- 24 18. G. Montavon; E. Alhajji; B. Grambow, *Environ. Sci. Technol.* **2006**, 40, 4672-4679.
- 25 19. L. R. Van Loon; B. Baeyens; M. H. Bradbury, *Appl. Geochem.* **2009**, 24, (5), 999-
26 1004.
- 27 20. L. R. Van Loon; M. A. Glaus, *Environ. Sci. Technol.* **2008**, 42, (5), 1600-1604.
- 28 21. F. T. Madsen, *Clay Miner.* **1998**, 33, 109-129.
- 29 22. L. Le Forestier; F. Muller; F. Villieras; M. Pelletier, *Appl. Clay Sci.* **2010**, 48, (1-2),
30 18-25.
- 31 23. M. Perronnet; F. Villieras; M. Jullien; A. Razafitianamaharavo; J. Raynal; D. Bonnin,
32 *Geochim. Cosmochim. Acta* **2007**, 71, (6), 1463-1479.
- 33 24. C. Tournassat; A. Neaman; F. Villiéras; D. Bosbach; L. Charlet, *Am. Mineral.* **2003**,
34 88, (2), 1989-1995.
- 35 25. S. Yokoyama; M. Kuroda; T. Sato, *Clay. Clay. Miner.* **2005**, 53, (2), 147-154.
- 36 26. C. Tournassat; E. Ferrage; C. Poinsignon; L. Charlet, *J. Colloid Interf. Sci.* **2004**, 273,
37 (1), 234-246.
- 38 27. I. C. Bourg; G. Sposito; A. C. M. Bourg, *J. Colloid Interf. Sci.* **2007**, 312, (2), 297-
39 310.
- 40 28. I. C. Bourg; G. Sposito, in: *Handbook of Soil Science, second edition*, 2011, in press.
- 41 29. G. Sposito, *Surface chemistry of soils*. Oxford University press: New York, 1984; p
42 223.
- 43 30. A. P. Vanselow; P. Albert, *Soil Sci.* **1932**, 33, (2), 95-114.
- 44 31. S. Y. Chu; G. Sposito, *Soil Sci. Soc. Am. J.* **1981**, 45, 1084-1089.
- 45 32. G. L. Gaines; H. C. Thomas, *J. Chem. Phys.* **1953**, 21, 714-718.
- 46 33. G. Sposito; K. M. Holtzclaw; C. T. Johnston; C. S. Le Vesque, *Soil Sci. Soc. Am. J.*
47 **1981**, 45, 1079-1084.
- 48 34. G. Sposito; S. V. Mattigod, *Clay. Clay. Miner.* **1979**, 27, (2), 125-128.

- 1 35. A. Maes; P. Peigneur; A. Cremers in: *Thermodynamics of transition metal ion*
2 *exchange in montmorillonite*, Proceedings of the International Clay Conference,
3 Wilmette, Illinois, USA, 1975; Applied Publishing Ltd.: Wilmette, Illinois, USA,
4 1975; pp 319-329.
- 5 36. P. Fletcher; G. Sposito, *Clay Miner.* **1989**, 24, 375-391.
- 6 37. M. H. Bradbury; B. Baeyens, *Geochim. Cosmochim. Acta* **2005**, 69, (22), 5391-5392.
- 7 38. M. H. Bradbury; B. Baeyens, *Geochim. Cosmochim. Acta* **2005**, 69, (4), 875-892.
- 8 39. C. Tournassat; H. Gailhanou; C. Crouzet; G. Braibant; A. Gautier; E. C. Gaucher, *Soil*
9 *Sci. Soc. Am. J.* **2009**, 73, (3), 928-942.
- 10 40. R. J. Lewis; H. C. Thomas, *J. Phys. Chem.* **1963**, 67, 1781-1783.
- 11 41. A. Banin, *Isr. J. Chem.* **1968**, 6, 27-36.
- 12 42. D. R. Lewis, *Clay. Clay. Miner.* **1952**, 1, 54-69.
- 13 43. M. B. McBride, *Clay. Clay. Miner.* **1980**, 28, (4), 255-261.
- 14 44. G. Sposito; C. Jouany; K. M. Holtzclaw; C. S. LeVesque, *Soil Sci. Soc. Am. J.* **1983**,
15 47, 1081-1085.
- 16 45. I. Shainberg; J. D. Oster; J. D. Wood, *Soil Sci. Soc. Am. J.* **1980**, 44, 960-964.
- 17 46. L. L. Schramm; J. C. T. Kwak, *Clay. Clay. Miner.* **1982**, 30, (1), 40-48.
- 18 47. A. Banin; N. Lahav, *Isr. J. Chem.* **1968**, 6, 235-250.
- 19 48. I. Shainberg; H. Otoh, *Isr. J. Chem.* **1968**, 6, 251-259.
- 20 49. N. Lahav; A. Banin, *J. Colloid Interf. Sci.* **1968**, 26, (2), 238-240.
- 21 50. T. Kozaki; J. H. Liu; S. Sato, *Phys. Chem. Earth* **2008**, 33, (14-16), 957-961.
- 22 51. T. Sato; T. Watanabe; R. Otsuka, *Clay. Clay. Miner.* **1992**, 40, 103-113.
- 23 52. Y. Horikawa; R. S. Murray; J. P. Quirk, *Colloid. Surface.* **1988**, 32, 181-195.
- 24 53. I. Sondi; V. Tomasic; N. Filipovic-Vincekovic, *Croat. Chem. Acta* **2008**, 81, (4), 623-
25 629.
- 26 54. C. Tournassat; Y. Chapron; P. Leroy; M. Bizi; F. Boulahya, *J. Colloid Interf. Sci.*
27 **2009**, 339, 533-541.
- 28 55. I. C. Bourg; G. Sposito, *J. Colloid Interf. Sci.* **2011**, 360, (2), 701-715.
- 29 56. M. L. Schlegel; K. L. Nagy; P. Fenter; L. Cheng; N. C. Sturchio; S. D. Jacobsen,
30 *Geochim. Cosmochim. Acta* **2006**, 70, (14), 3549-3565.
- 31 57. D. A. Dzombak; R. J. M. Hudson, in: *Aquatic Chemistry. Interfacial and interspecies*
32 *processes*, C. P. Huang; C. O'Melia; J. J. Morgan, (Eds.) 1995; Vol. 244, pp 59-94.
- 33 58. C. A. J. Appelo; L. R. Van Loon; P. Wersin, *Geochim. Cosmochim. Acta* **2010**, 74,
34 (4), 1201-1219.
- 35 59. M. Borkovec; J. Westall, *J. Electroanal. Chem.* **1983**, 150, (1-2), 325-337.
- 36 60. C. A. J. Appelo; P. Wersin, *Environ. Sci. Technol.* **2007**, 41, 5002-5007.
- 37 61. P. Leroy; A. Revil, *J. Geophys. Res. Sol-Ea.* **2009**, 114, -.
- 38 62. P. Leroy; A. Revil; S. Altmann; C. Tournassat, *Geochim. Cosmochim. Acta* **2007**, 71,
39 (5), 1087-1097.
- 40 63. I. Shainberg; W. D. Kemper, *Soil Sci.* **1967**, 103, (1), 4-9.
- 41 64. M. J. Avena; C. De Pauli, *J. Colloid Interf. Sci.* **1998**, 202, 195-204.
- 42 65. P. Leroy; A. Revil, *J. Colloid Interf. Sci.* **2004**, 270, (2), 371-380.
- 43 66. S. S. Lee; P. Fenter; C. Park; N. C. Sturchio; K. L. Nagy, *Langmuir* **2010**, 26, (22),
44 16647-16651.
- 45 67. B. Rotenberg; V. Marry; J.-F. Dufrêche; E. Giffaut; P. Turq, *J. Colloid Interf. Sci.*
46 **2007**, 309, (2), 289-295.
- 47 68. D. A. Dzombak; F. M. M. Morel, *Surface complexation modeling-Hydrous ferric*
48 *oxide*. New York, 1990; p 393.

- 1 69. D. L. Parkhurst; C. A. J. Appelo **1999**, *User's guide to PHREEQC (Version 2) - A*
2 *computer program for speciation, batch-reaction, one-dimensional transport, and*
3 *inverse geochemical calculations*;
- 4 70. D. Vantelon; E. Montarges-Pelletier; L. J. Michot; V. Briois; M. Pelletier; F. Thomas,
5 *Phys. Chem. Miner.* **2003**, 30, (1), 44-53.
- 6 71. D. Vantelon; M. Pelletier; L. Michot; O. Barrès; F. Thomas, *Clay Miner.* **2001**, 36,
7 369-379.
- 8 72. P. Bar On; I. Shainberg; I. Michaeli, *J. Colloid Interf. Sci.* **1970**, 33, (3), 471-472.
- 9 73. I. Sondi; J. Biscan; V. Pravdic, *J. Colloid Interf. Sci.* **1996**, 178, (2), 514-522.
- 10 74. M. Duc; F. Gaboriaud; F. Thomas, *J. Colloid Interf. Sci.* **2005**, 289, (1), 148-156.
- 11 75. J. C. Rémy; L. Orsini, *Sciences du Sol* **1976**, 4, 269-275.
- 12 76. R. Dohrmann; S. Kaufhold, *Clay. Clay. Miner.* **2009**, 57, (3), 338-352.
- 13 77. K. Verburg; P. Baveye, *Clay. Clay. Miner.* **1994**, 42, (2), 207-220.
- 14 78. E. Tertre; D. Pret; E. Ferrage, *J. Colloid Interf. Sci.* **2011**, 353, (1), 248-256.
- 15 79. I. Shainberg; N. I. Alperovitch; R. Keren, *Clay. Clay. Miner.* **1987**, 35, (1), 68-73.
- 16 80. G. Sposito; K. M. Holtzclaw; L. Charlet; C. Jouany; A. L. Page, *Soil Sci. Soc. Am. J.*
17 **1983**, 47, 51-56.
- 18 81. G. Sposito; K. M. Holtzclaw; C. Jouany; L. Charlet, *Soil Sci. Soc. Am. J.* **1983**, 47, (5),
19 917-921.
- 20 82. L. Tang; D. L. Sparks, *Soil Sci. Soc. Am. J.* **1993**, 57, 42-46.
- 21 83. P. M. Kopittke; H. B. So; N. W. Menzies, *Eur. J. Soil Sci.* **2006**, 57, (5), 626-633.
- 22 84. R. P. T. Janssen; M. G. M. Bruggenwert; W. H. van Riemsdijk, *Eur. J. Soil Sci.* **2003**,
23 54, (2), 335-345.
- 24 85. R. Van Bladel; G. Gavia; H. Laudelout in: *A comparison of the thermodynamic,*
25 *double layer theory and empirical studies of the Na-Ca exchange equilibria in clay*
26 *water systems*, Proceedings of the international clay conference Madrid, Spain, 1972;
27 Madrid, Spain, 1972.
- 28 86. A. Maes; A. Cremers, *J. Chem. Soc., Faraday Trans.* **1977**, 73, 1807-1814.
- 29 87. B. Baeyens; M. H. Bradbury **1995**, *A quantitative mechanistic description of Ni, Zn*
30 *and Ca sorption on Na-montmorillonite. Part II. sorption measurements.*; Paul
31 Scherrer Institut. PSI-Bericht Nr. 95-11:
- 32 88. H. Ciesielski; T. Sterckeman, *Agronomie* **1997**, 17, 9-16.
- 33 89. H. Ciesielski; T. Sterckeman, *Agronomie* **1997**, 17, 1-7.
- 34 90. G. Sposito, *Soil Sci. Soc. Am. J.* **1991**, 55, (4), 965-967.
- 35 91. L. Charlet; C. Tournassat, *Aquat. Geoch.* **2005**, 11, (2), 115-137.
- 36 92. E. Ferrage; C. Tournassat; E. Rinnert; L. Charlet; B. Lanson, *Clay. Clay. Miner.* **2005**,
37 53, (4), 348-361.
- 38 93. A. V. Blackmore; R. D. Miller, *Soil Sci. Soc. Proc.* **1961**, 25, 169-173
- 39 94. R. S. B. Greene; A. M. Posner; J. P. Quirk, *Soil Sci. Soc. Am. J.* **1973**, 37, 457-460.
- 40 95. C. Tournassat; C. A. J. Appelo, *Geochim. Cosmochim. Acta* **2011**, 75, (13), 3698-
41 3710.
- 42 96. T. Melkior; E. C. Gaucher; C. Brouard; S. Yahiaoui; D. Thoby; C. Clinard; E. Ferrage;
43 D. Guyonnet; C. Tournassat; D. Coelho, *J. Hydr.* **2009**, 370, (1-4), 9-20.
- 44
45